J Mol Model (2015) 21:51
DOI 10.1007/s00894-015-2607-3

ORIGINAL PAPER

# Mechanical properties of chiral and achiral silicon carbide nanotubes under oxygen chemisorption

**R. Ansari · M. Mirnezhad · M. Hosseinzadeh**

Received: 13 October 2014 / Accepted: 1 February 2015


**Abstract** In this paper, the mechanical properties of fully oxygenated silicon carbide nanotubes ($O_2$-SiCNTs) are explored using a molecular mechanics model joined with the density functional theory (DFT). The closed-form analytical expressions suggested in this study can easily be adapted for nanotubes with different chiralities. The force constants of molecular mechanics model proposed herein are derived through DFT within a generalized gradient approximation. Moreover, the mechanical properties of fully oxygenated silicon carbide ($O_2$-SiC) sheet are evaluated for the case that the oxygen atoms are adsorbed on one side of the SiC sheet. According to the results obtained for the bending stiffness of $O_2$-SiC sheet, one can conclude that the $O_2$-SiC sheet has isotropic characteristics.

**Keywords** Density functional theory · Mechanical properties · Molecular mechanics model · Oxygenated silicon carbide sheet · Oxygenated silicon carbide nanotubes

## Introduction

Silicon carbide-based materials, owing to have superlative physical properties such as high hardness, excellent thermal stability, and heat conductivity [1–3], have drawn great interest from both academia and industry in recent years [4, 5].

The simplest tubular forms of SiC, i.e., SiCNTs were experimentally synthesized via the reaction of SiO with multi-walled carbon nanotubes (MWCNTs) [6]. Recently, through first-principles calculations it was revealed that the single-walled SiCNTs (SWSiCNTs) have superior properties in comparison to single-walled carbon nanotubes in several aspects [7–17].

Owing to the difference in the electronegativities of C and Si atoms, SiCNTs are polar materials while on the contrary carbon nanotubes (CNTs) are non-polar. Moreover, the covalent bond length in SiC (1.80 Å) is larger than those of B-N (1.44 Å) and C-C (1.42 Å). As a result, SiCNTs are better candidates compared to boron nitride nanotubes (BNNTs) and CNTs for applications involving materials storage [18]. Meanwhile, theoretical studies revealed that SiCNTs due to their polar nature exhibit better reactivity than CNTs [11].

Some other studies have also been conducted to investigate the properties of SiCNTs [10, 19–30]. To mention some of these works Baumeier et al. [10] who studied the structural, elastic, and electronic properties of SiCNTs via ab initio methods, Zheng and Lowther [19] who investigated numerically the mechanical properties of SiCNTs and Khani et al. [21] who discussed the vibrational behavior of SiCNTs. In addition, Dai and his associates [23] investigated the structural and electronic properties of N, P, As, and Sb doped (9.0) SWSiCNTs via the firs-principle theory. Alfieri and Kimoto [25] performed an *ab anitio* study and showed how hydrogen overcome the metastability of SiCNTs.

The interaction between $O_2$ and SiCNTs is an important issue which needs considerable attention especially when SiCNTs are upon air exposure. Nevertheless, the number of studies devoted to the effect of $O_2$ on SiCNTs is very limited in the literature [31–33]. For instance, Szabó and Gali [31] investigated the SiC oxidization phenomenon in the presence of oxygen through ab initio DFT calculations. Their results showed that the structure of SiCNTs remains unchanged in ambient oxygen. In addition, they demonstrated that the $O_2$ molecules dissociate as interstitials on SiCNTs even at room temperature. Cao et al. [32] applied DFT to explore the

R. Ansari (✉) · M. Mirnezhad · M. Hosseinzadeh (✉)
Department of Mechanical Engineering, University of Guilan, P.O. Box 3756, Rasht, Iran
e-mail: r_ansari@guilan.ac.ir
e-mail: mhdshhosseinzadeh@gmail.com

Published online: 19 February 2015

adsorption/dissociation of the $O_2$ molecule on the surface of SiCNTs. In their investigation, several adsorption configurations such as chemisorptions and cycloaddition configurations were found for triplet and singlet $O_2$. Ganji and Ahaz [33] studied the binding of molecular oxygen to a (5,0) SWSiCNT by density functional calculations. They tested the stability of $O_2$-SiCNT via ab initio molecular dynamics simulation at room temperature. Their findings revealed that adsorptive capability of SiCNTs is higher than that of CNTs.

According to the discussion presented in the previous paragraph, it can be concluded that the adsorbed-$O_2$ molecules may be detrimental to the mechanical properties of SiCNTs. Hence, more investigations are required to study the effect of $O_2$ on SiCNTs for all the possible usage of these nanostructures. For this purpose, the mechanical properties of the fully oxygenated SWSiCNTs and SiC sheet are investigated in this work in which the oxygen atoms are adsorbed on one side of the unwrapped SiC sheet. Using a molecular mechanics model, closed-form expressions are derived to obtain size- and chirality-dependent mechanical properties of $O_2$-SiCNTs and $O_2$-SiC sheet such as surface Young's modulus and Poisson's ratio. These expressions can be successfully applied to SiCNTs with different chiralities including armchair, zigzag, and also chiral. In addition, DFT is utilized in order to calculate the force constants of molecular mechanics theory.

## Molecular mechanics model

While quantum mechanics methods have proven their efficiency in calculating the potential energy of nanostructured materials via the electronic structure of molecule, they lack a priori concept of chemical bonds. Molecular mechanics methods are more efficient approaches in this respect. In molecular mechanics methods, the potential energy of the system is determined without invoking any description of quantum mechanics. The Born-Oppenheimer approximation which is the basis of molecular mechanics model allows one to describe the motions of electrons and the motions of nuclei independently. Moreover, unlike quantum mechanics methods, in molecular mechanics model the motions of nuclei are studied and electrons are implicitly included in the calculations which are assumed to find their optimum distribution around the nuclei.

As aforementioned, calculations of potential energy within molecular mechanics methods outweigh in some aspects compared to quantum mechanics approaches. It should be noted that the comparison between these two approaches, for more complex structures such as nanotubes, especially ones with different chiralities shows that the molecular mechanics methods are much faster and highly reliable. Additionally, the use of quantum methods for complex structures which contain a large number of atoms is computationally inefficient and somewhat unworkable [34], so this is something which requires high computational effort for calculating the potential energy of any special state. In other words, with the aid of molecular mechanics methods which are highly accurate and fast, similar results with ones from quantum mechanics approaches can be obtained with less computational effort. In this regard, a molecular mechanics model is suggested in this study to determine the Young's modulus and Poisson's ratio of $O_2$-SiCNTs. Note that the atomistic demonstration of $O_2$-SiCNT is shown in Fig. 1.

In a molecular system, the total potential energy which is the sum of individual potential components can be written in the following form:

$$E_t = E_\rho + E_\theta + E_\omega + E_\tau + E_{vdw} + E_{es}. \quad (1)$$

$E_\rho$, $E_\theta$, $E_\omega$, $E_\tau$ in the above equation denote the bond stretching, bond angle variation, bond inversion, and bond

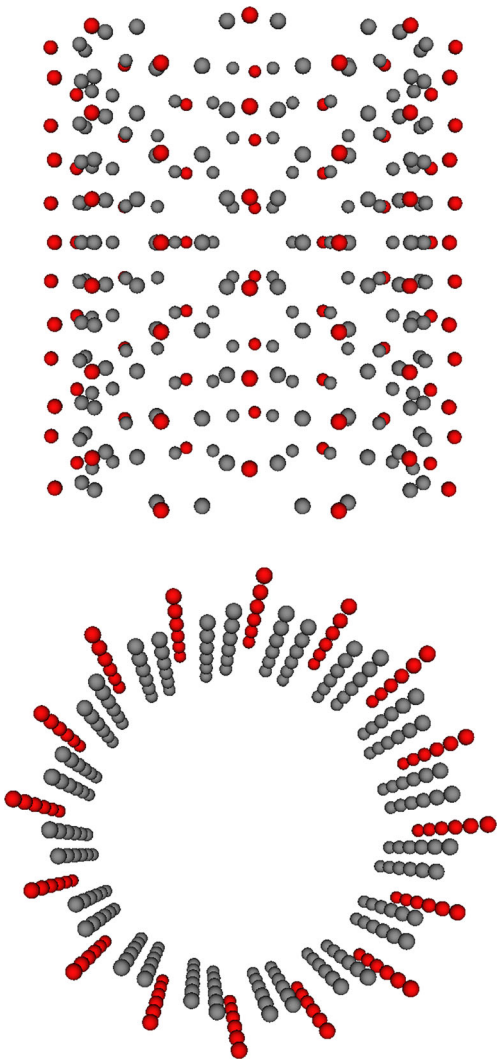

**Fig. 1** Top and side view of oxygenated SiC sheet in tubular form (atomistic view)

torsion energies, respectively. The other two terms, i.e., $E_{vdw}$ and $E_{es}$, represent the van der Waals and electrostatic interactions, respectively. Depending on the different materials and loading conditions, different functional forms can be used for the energy terms in Eq. (1). In some cases, such as the present analysis, it is expected that $E_\rho$ and $E_\theta$ to be the dominant terms in contrast to the other remaining terms.

Hook's law with adequate efficiency and accuracy is frequently used to define the interactions between bound atoms, thus, the total energy of the system can be written as:

$$E_t = \sum \frac{1}{2} K_\rho (dr)^2 + \sum \frac{1}{2} C_\theta (d\theta)^2 \quad , \tag{2}$$

in which $dr$ is the bond elongation and $d\theta$ is the bond angle variance. $K_\rho$ and $C_\theta$ are the force constants representing the energies associated with the bond stretching and the bond angle variation, respectively.

As seen from Fig. 2, for an atom indexed by $ij$ in a SiCNT three bond lengths $r_{ij1}$, $r_{ij2}$, $r_{ij3}$ and three bond angles $\theta_{ij1}$, $\theta_{ij2}$, $\theta_{ij3}$ are attributed.

To obtain the equilibrium equations an effective "stick-spiral" model is employed. In the effective "stick-spiral" model an elastic stick with an axial stiffness of $K_\rho$ and infinite bending stiffness is used to model the force-stretch relationship of the Si-C bond. The reason for considering infinite bending stiffness is due to the fact that the chemical bonds always remain straight regardless of the applied load. Moreover, a spiral spring with a finite torsional stiffness of $C_\theta$ is used to model the twisting moment caused by angular variation of bond angle. It should be noted that in the proposed molecular mechanics model it is assumed the hexagonal structure of nanotubes remains intact after oxygen adsorption occurs in the SiCNT. Thus, to incorporate the influences of oxygen adsorption into the model, the proper values of force constants will be obtained within DFT.

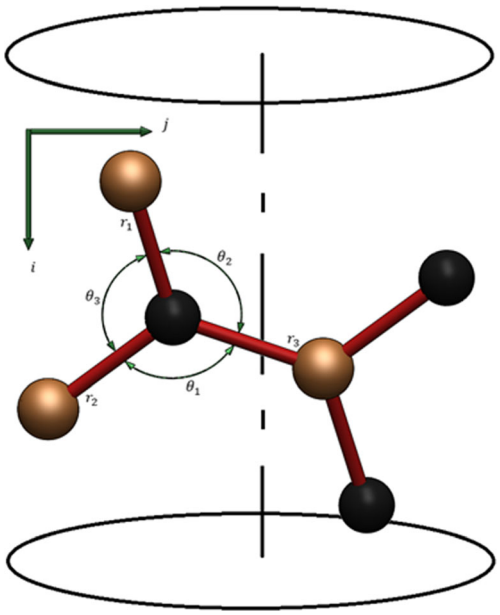


**Fig. 2** Definition of atom position in a chiral nanotube

The closed-form expressions for surface Young's modulus and Poisson's ratio of a chiral nanotube can be defined as [35]:

$$Y_s = \frac{1}{2\pi R}\left(\frac{(n+m)K_\rho r_1}{\sin\left(\frac{\pi}{3}+\Theta\right)\sin\left(\frac{\theta_3}{2}\right)\left(\frac{\lambda_A K_\rho r_2^1}{C_\theta \tan\left(\frac{\theta_3}{2}\right)^2}+1\right)}\right) \tag{3}$$

$$\upsilon = -\frac{\cos\left(\frac{\theta_3}{2}\right)\left(1-\frac{\lambda_A K_\rho r_1^2}{C_\theta}\right)}{\left(1+\cos\left(\frac{\theta_3}{2}\right)\right)\left(\frac{\lambda_A K_\rho r_1^2}{C_\theta \tan\left(\frac{\theta_3}{2}\right)^2}+1\right)} \quad , \tag{4}$$

where $\theta$ represents the chiral angle and $R = \frac{r_0\sqrt{3(n^2+nm+m^2)}}{2\pi}$ is the radius of nanotube. Note that $r_0$ is the Si–C bond length. Note that in order to employ the molecular mechanic method, and also for the aim of simplicity, equality is considered for the values of bond lengths as given in Table 1.

$$\lambda_A = \frac{\sin(\theta_2)\cot\left(\frac{\theta_3}{2}\right)}{4\sin(\theta_2)\cot\left(\frac{\theta_3}{2}\right)-2\sin\left(\frac{\theta_3}{2}\right)\cot(\theta_2)\cos\left(\frac{\pi}{n+m}\right)} \tag{5}$$

It is worth mentioning that in order to avoid the ambiguity in the definition of wall thickness of nanotubes, in this study the surface Young's modulus is used which is obtained by multiplying the conventional Young's modulus by the nanotube wall thickness.

As can be deduced, the bond angles $\theta_3$ and $\theta_2$ in the undeformed configuration of a chiral nanotube are equal to $2\pi/3$. By letting $n$ approaches infinity in Eqs. (3) and (4), the expressions for surface Young's modulus and Poisson's ratio of a SiC sheet are given by [36]:

$$Y_S = \frac{8\sqrt{3}K_\rho}{\frac{K_\rho r_1^2}{C_\theta}+18} \tag{6}$$

**Table 1** Properties of the $O_2$-SiC sheet

| Surface Young's modulus (GPa nm) | Poisson's ratio | Lattice constant (nm) | Si–C bond length (nm) | O–Si adsorption bond length (nm) | O–C adsorption bond length (nm) |
|---|---|---|---|---|---|
| 126 | 0.32 | 0.266 | 0.186 | 0.167 | 0.158 |

$$\upsilon = \frac{\frac{K_\rho r_1^2}{C_\theta} - 6}{\frac{K_\rho r_1^2}{C_\theta} + 18} \quad . \tag{7}$$

## Results and discussion

In this section, the mechanical properties of $O_2$-SiCNTs with different types of chiralities are investigated using a proposed molecular mechanics model within the DFT framework. In order to accurately estimate the force constants ($K_\rho$ and $C_\theta$) of Eq. (2) the generalized gradient approximation is used for the exchange correlation of Perdew-Burke-Ernzerhof (PBE) [37, 38]. Meanwhile, the DFT calculations are performed to determine the magnitudes of surface Young's modulus, Poisson's ratio, bending stiffness and atomic structure of $O_2$-SiC sheet. Note that all the simulations in this study are carried out using Quantum-Espresso code [39]. To avoid the ambiguity of sophisticated conditions, in the present analysis the smallest hexagonal unit cell is chosen. This assumption is based on the fact that increasing the unit cell dimensions do not considerably affects the obtained results [40]. Moreover, Brillouin zone integration is executed using a Monkhorst-Pack [41] *k*-point mesh of 12×12×12 and the plane-wave cut-off energy for wave functions is taken as 60 Ry.

The most stable state of oxygen adsorption on the SiC sheet is illustrated in Fig. 3. According to this figure, the adsorption of oxygen atoms on silicon and carbon atoms occurs at one side of SiC sheet. Notably, the structure illustrated in Fig. 3 is apparently the starting point of oxygen adsorption phenomenon in which the structure is not relaxed yet. In other words, the relaxed configuration is slightly different. As known, although the oxygen adsorption phenomenon changes the atomic structure of the SiC sheet, but it is assumed that the atomic structure remains unchanged after the oxygen atoms are adsorbed via SiC sheet.

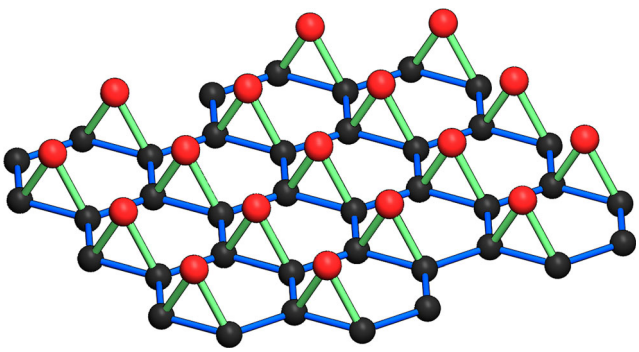

**Fig. 3** Stable state of oxygen adsorption on SiC sheet

This assumption enables one to employ Eqs. (3) and (4) for the mechanical properties of $O_2$-SiCNTs on the basis of the molecular mechanics approach. To include the effect of adsorbed oxygen atoms, the force constants are determined. To this end, the strain energy derived from DFT is equated with that from molecular mechanics method. Moreover, it is worth mentioning that as long as the strain energy calculations are in the harmonic elastic deformation range, and hence the applied strain is small, it can be assumed that the initial hexagonal structure of SiC sheet is maintained.

The alteration of strain energy versus the axial strain for $O_2$-SiC sheet is illustrated in Fig. 4. It is worth mentioning that the strain energy calculations are performed for the harmonic elastic deformation regime. Accordingly, since the harmonic zone for strain is taken between $-0.02<\varepsilon<0.02$, it is acceptable to consider that the hexagonal structure of SiC sheet is kept unchanged.

Using the DFT calculations and applying the relations of $Y_s=(1/A_0)\times(\partial^2 E_S/\partial\varepsilon^2)$ ($A_0$ denotes the equilibrium area of the system) and $\upsilon=-\varepsilon_{trans}/\varepsilon_{axial}$ (the ratio of the transverse strain to the axial strain) for the surface Young's modulus and Poisson's ratio, respectively, the mechanical properties of $O_2$-SiC sheet is given in Table 1. In this table, the values of

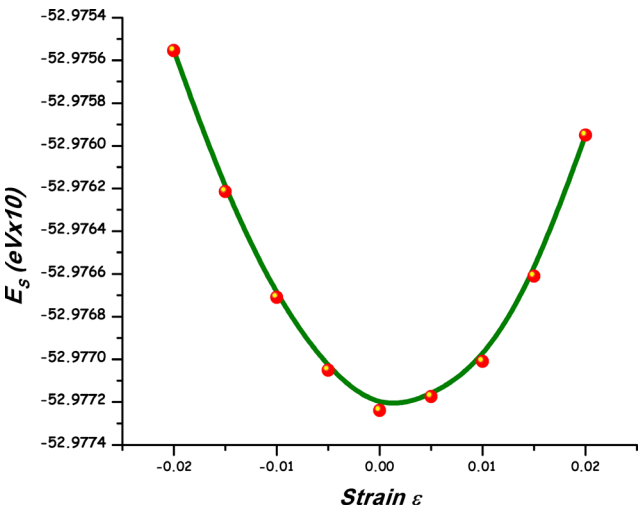


**Fig. 4** Alteration of strain energy $E_S$ versus axial strain for the $O_2$-SiC sheet

lattice constant and bond lengths of oxygenated SiC sheet are also listed. According to this table, the surface Young's modulus of $O_2$-SiC sheet obtained in this paper is 24.1 % smaller than that of calculated in [40] for the pure SiC sheet. This finding clearly signifies that the oxygen adsorption has a destructive influence on the mechanical properties of SiC-based nanostructures. Moreover, in order to calculate the bending stiffness of $O_2$-SiC sheets, they are wrapped into nanotubes along different directions. The style of wrapping $O_2$-SiC sheets is denoted by a pair of indices ($n$, $m$). In addition, when the SiC sheets are wrapped to form the SiCNTs, the adsorbed oxygen atoms can be either inside or outside of the SiCNTs. By keeping this in mind, the alteration of strain energy per atom with respect to the bending curvature is depicted in Fig. 5. According to this figure, the strain energies per atom

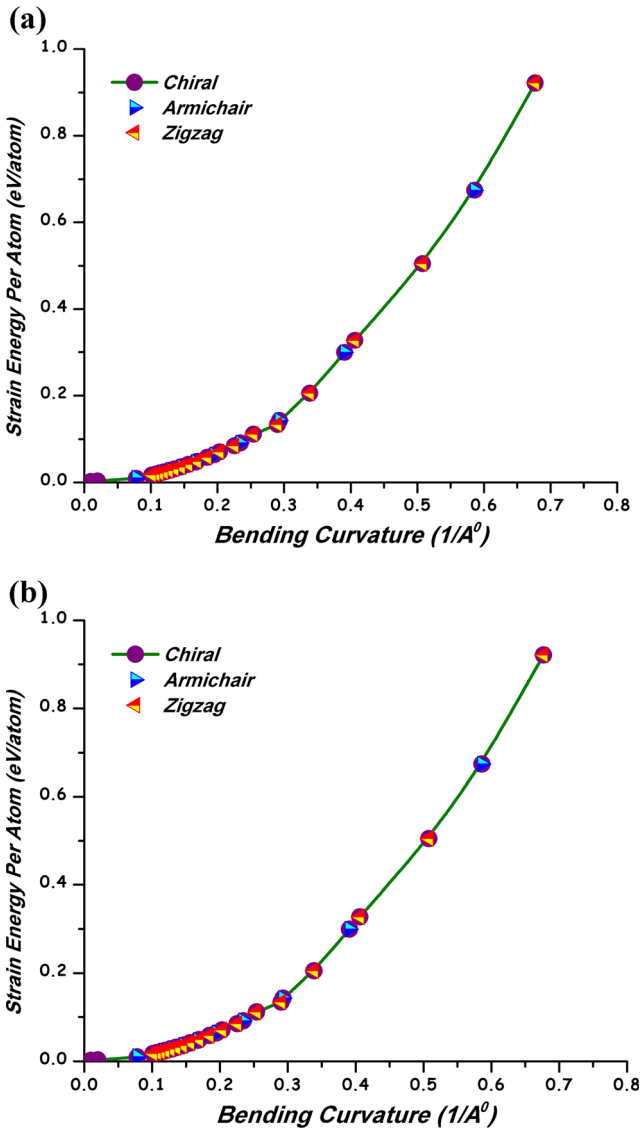


**Fig. 5** Alteration of strain energy per atom versus bending curvature of the $O_2$-SiC sheet. **a** The oxygen atoms are adsorbed on the inside of SiCNT. **b** The oxygen atoms are adsorbed on the outside of SiCNT

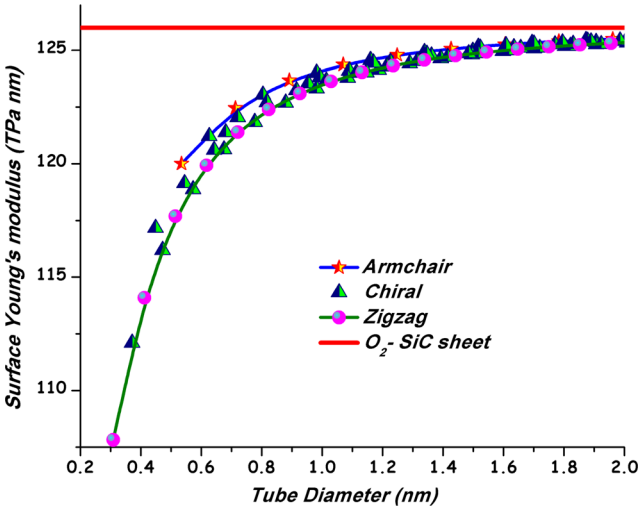


**Fig. 6** Alteration of surface Young's modulus of the $O_2$-SiCNTs for different types of chiralities versus tube diameter

for fully relaxed wrapped $O_2$-SiC sheets for armchair, zigzag, and chiral orientations are the same. This clearly points out that the direction of wrapping does not have any influence on the results. Thus, it is already proved that the chirality has no effect on the bending stiffness. In other words, it can be concluded that $O_2$-SiC sheets are isotropic. Also, the values of bending stiffness for the cases that the oxygen adsorption occurs inside and outside of the SiCNT are obtained as 0.396 eV and 0.377 eV, respectively. These values which are obtained by differentiating twice the strain energy with respect to the bending curvature indicate that the direction of oxygen atoms on the SiCNT affects the bending stiffness in which when the oxygen atoms are inside the SiCNT the bending stiffness is found to be larger compared to the case when they are outside the SiCNT.

Molecular mechanics theory as stated beforehand acts as a means for computing those molecular properties which do not

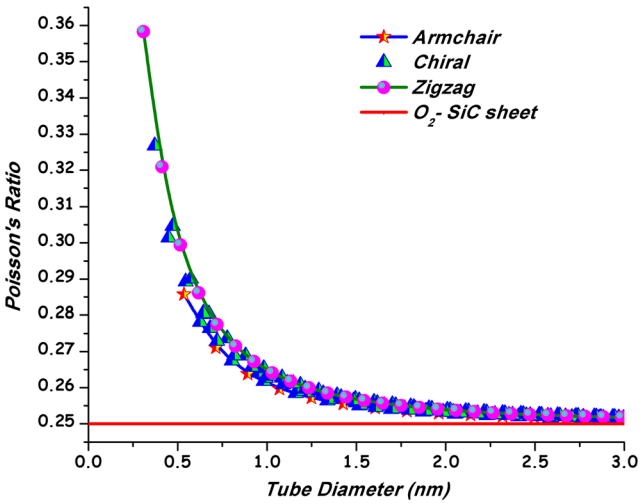


**Fig. 7** Alteration of poisson's ratio of the $O_2$-SiCNTs for different types of chiralities versus the tube diameter

depend on the electronic structure and only takes into account the physicochemical interactions. Hence, the calculations performed to determine the potential energy are fast and efficient. As long as these calculations are done without including the effects of the electronic structure, the accuracy of the prediction might be lost. Therefore, in order to increase the accuracy of the results a relation between molecular mechanics and DFT is needed. For this aim, the force constants of molecular mechanics model ($K_\rho$ and $C_\theta$) are introduced which are obtained through establishing a linkage between the individual energy terms from molecular mechanics and the strain energy calculated from DFT. Accordingly, the effects of electronic structure are incorporated into the calculations which can improve the accuracy of the results obtained within the molecular mechanics model.

By substituting the values of surface Young's modulus and Poisson's ratio of the $O_2$-SiC sheet into Eqs. (6) and (7) the values of 290.984 nN/nM and 0.724 nN nm are obtained for $K_\rho$ and $C_\theta$, respectively. Now, by applying the calculated force constants $K_\rho$ and $C_\theta$ into Eq. (3), the values of surface Young's modulus of the $O_2$-SiCNTs with various types of chiralities can be evaluated. As seen from Fig. 6, surface Young's moduli of armchair, zigzag, and chiral $O_2$-SiCNTs are plotted versus the tube diameter. When a large value is chosen for the diameter of $O_2$-SiCNT, the curvature of the tube approaches zero, hence, in this case the $O_2$-SiCNT can be considered as an $O_2$-SiC sheet. As shown in Fig. 6, the surface Young's modulus of $O_2$-SiC sheet is constant with respect to the diameter. With a closer look to this figure, it is observed that as the diameter of $O_2$-SiCNT increases their corresponding surface Young's moduli tend to that of $O_2$-SiC sheet for all types of chiralities CM7. In addition, it can be concluded that for all values of tube diameters, the values of surface Young's modulus of chiral $O_2$-SiCNTs are between those of armchair and zigzag $O_2$-SiCNTs, in which the values for armchair $O_2$-SiCNTs are highest.

Poisson's ratios of the $O_2$-SiCNTs with various types of chiralities are calculated through Eq. (4) by substituting the values of force constants obtained from DFT. The alterations of Poisson's ratio corresponding to armchair, zigzag, and chiral $O_2$- SiCNTs against tube diameter are depicted in Fig. 7. This figure clearly shows that as the tube diameter decreases the values of Poisson's ratio decrease. As seen from this figure, when the tube curvature approaches zero its effect on the Poisson's ratio is similar to that discussed formerly for the surface Young's modulus. Moreover, for all values of the tube diameter, the values of Poisson's ratios for armchair $O_2$-SiCNTs are lower than those of zigzag $O_2$-SiCNTs. All these findings clearly show that for the smaller values of the tube diameter the influence of chirality is more pronounced on the mechanical properties of $O_2$-SiCNTs.

## Conclusions

In this paper, the mechanical properties of $O_2$-SiC sheet and achiral and chiral $O_2$-SiCNTs including surface Young's modulus, Poisson's ratio, and bending stiffness were investigated using a molecular mechanics model. The method used in this study compensates the inability of molecular mechanics model in accounting for the electronic structures of the system. For this aim, the force constants of molecular mechanics theory were obtained successfully using DFT within a generalized gradient approximation. This success can be regarded as a basis for further exploring different features of oxygenated SiCNTs using molecular mechanics.

The bending stiffness of $O_2$-SiC sheet was obtained for two cases; in the first case it was considered that the oxygen atoms are adsorbed from inside of the SiCNT whereas in the second case it was assumed that the oxygen adsorption occurs outside the SiCNT. In addition, it was observed that as the tube diameter of $O_2$-SiCNTs increases the surface Young's modulus increases while the Poisson's ratio decreases. Further, when a large value is chosen for the tube diameter the mechanical properties of $O_2$-SiCNTs tend to those of $O_2$-SiC sheet. Finally, it was concluded that for all values of the tube diameter the values of Young's modulus of armchair $O_2$-SiCNTs are larger than those of chiral $O_2$-SiCNTs, and zigzag $O_2$-SiCNTs have the minimum values among the given cases. However, a reverse trend was observed for the variation of Poisson's ratio with regard to chirality.

## References

1. Choyke WJ, Matsunami H, Pensl G (2004) Silicon carbide: recent major advances. Springer, Berlin
2. Chelnokov VE, Syrkin AL (1997) High temperature electronics using SiC: actual situation and unsolved problems. Mater Sci Eng B 46:248–2531997
3. Porter LM, Davis RF (1995) A critical review of ohmic and rectifying contacts for silicon carbide. Mater Sci Eng B 34:83–105
4. Huang HC, Ghoniem N (1993) Neutron displacement damage cross sections for SiC. J Nuclea Mate 199:221–230
5. Yang W, Araki H, Tang C, Thaveethavorn S, Kohyama A, Suzuki H, Noda T (2005) Single-crystal SiC nanowires with a thin carbon coating for stronger and tougher ceramic composites. Adv Mater 17: 1519–1523
6. Sun XH, Li CP, Wong WK, Wong NB, Lee CS, Lee ST, Teo BT (2002) Formation of silicon carbide nanotubes and nanowires via reaction of silicon (from disproportionation of silicon monoxide) with carbon nanotubes. J Am Chem Soc 124: 14464–14471
7. Miyamoto Y, Yu BD (2002) Computational designing of graphitic silicon carbide and its tubular forms. Appl Phys Lett 80:586–588
8. Mavrandonakis A, Froudakis GE, Schnell M, Mühlhäuser M (2003) From pure carbon to silicon−carbon nanotubes: an ab-initio study. Nano Lett 3:148–1484

9. Menon M, Richter E, Mavrandonakis A, Froudakis G, Andriotis AN (2004) Structure and stability of SiC nanotubes. Phys Rev B 69: 115322–115325
10. Baumeier B, Kruger P, Pollmann J (2007) Structural, elastic, and electronic properties of SiC, BN, and BeO nanotubes. Phys Rev B 76:085407–085416
11. Mpourmpakis G, Froudakis G, Lithoxoos G, Samios J (2006) SiC Nanotubes: a novel material for hydrogen storage. Nano Lett 6:1581–1583
12. Gali A (2006) Ab initio study of nitrogen and boron substitutional impurities in single-wall SiC nanotubes. Phys Rev B 73:245415–245423
13. Shen H (2007) MD simulations on the melting and compression of C, SiC and Si nanotubes. J Mater Sci 42:6382–6387
14. Huang SP, Wu DS, Hu JM, Zhang H, Xie Z, Hu H, Chen WD (2007) First-principles study: size- dependent optical properties for semiconducting silicon carbide nanotubes. Opt Express 15:10947–10957
15. He RA, Chu ZY, Li XD, Si YM (2008) Synthesis and hydrogen storage capacity of SiC nanotube. Key Eng Mater 368–372:647–649
16. Wu IJ, Guo GY (2007) Optical properties of SiC nanotubes: an ab initio study. Phys Rev B 76:035343–035351
17. Wu IJ, Guo GY (2008) Second-harmonic generation and linear electro-optical coefficients of SiC polytypes and nanotubes. Phys Rev B 78:035447–035456
18. Zhang JM, Chen LY, Wang SF, Xu KW (2010) Comparison of the structural, electronic and magnetic properties of Fe, Co and Ni nanowires encapsulated into silicon carbide nanotube. Eur Phys J Cond Mat Comp Syst 73:555–561
19. Zheng B, Lowther JE (2010) Numerical investigations into mechanical properties of hexagonal silicon carbon nanowires and nanotubes. Nanoscale 2:1733–1739
20. Huda MN (2014) SiC nanostructures from a theoretical perspective. Rev Nanosci Nanotechnol 3:88–106
21. Khani N, Fakhrabadi MMS, Vahabi M, Kamkari B (2014) Modal analysis of silicon carbide nanotubes using structural mechanics. Appl Phys A 116:1687–1694
22. Xu B, Ouyang J, Xu Y, Wu MS, Liu G, Ouyang CY (2013) The structural, mechanical and electronic properties of (4, 4) SiC/C nanotube heterojunction: a first-principles study. Comput Mat Sci 68:367–370
23. Dai J, Chen D, Li Q (2014) First-principle study on the X (X = N, P, As, Sb) doped (9.0) single-walled SiC nanotubes. Phys Cond Mat 447:56–61
24. Andrievski RA (2009) Nano-sized silicon carbide: synthesis, structure and properties. Rus Chem Rev 78:821–831
25. Alfieri G, Kimoto T (2014) Ab initio prediction of SiC nanotubes with negative strain energy. Appl Phys Lett 104:033107
26. Zhang Y, Huang H (2008) Stability of single-wall silicon carbide nanotubes – molecular dynamics simulations. Comput Mat Sci 43: 664–669
27. Akbarpour MR, Salahi E, Alikhani Hesari F, Simchib A, Kim HS (2013) Fabrication, characterization and mechanical properties of hybrid composites of copper using the nanoparticulates of SiC and carbon nanotubes. Mater Sci Eng A 572:83–90
28. Joshi R, Engstler J, Haridoss P, Schneider JJ (2009) Formation of carbon nanotubes from a silicon carbide/carbon composite. Solid State Sci 11:422–427
29. Keller N, Pham-Huu C, Ehret G, Keller V, Ledoux MJ (2003) Synthesis and characterisation of medium surface area silicon carbide nanotubes. Carbon 41:2131–2139
30. Taguchi T, Igawa N, Yamamoto H, Jitsukawa S (2005) Synthesis of silicon carbide nanotubes. J Am Ceram Soc 88:459–461
31. Szabó Á, Gali A (2009) Effect of oxygen on single-wall silicon carbide nanotubes studied by first-principles calculations. Phys Rev B 80:075425–075431
32. Cao F, Xu X, Ren W, Zhao C (2010) Theoretical study of O2 molecular adsorption and dissociation on silicon carbide nanotubes. J Phys Chem C 114:970–976
33. Ganji MD, Ahaz B (2010) First principles simulation of molecular oxygen adsorption on SiC nanotubes. Commun Theor Phys 53:742–748
34. Sun QP, Tong P. IUTAM symposium on size effects on material and structural behavior at microns and nanoscales, solid mechanics and its applications, Springer
35. Mirnezhad M, Ansari R, Rouhi H (2012) Effects of hydrogen adsorption on mechanical properties of chiral single-walled zinc oxide nanotubes. J Appl Phys 111:014308–014318
36. Chang T, Gao H (2003) Size-dependent elastic properties of a single-walled carbon nanotube via a molecular mechanics model. J Mech Phys Solid 51:1059–1074
37. Perdew JP, Burke K, Ernzerhof M (1996) Generalized gradient approximation made simple. Phys Rev Lett 77:3865–3868
38. Perdew JP, Burke K, Wang Y (1996) Generalized gradient approximation for the exchange-correlation hole of a many-electron system. Phys Rev B 54:16533–16539
39. Baroni S, Corso DA, Gironcoli S, Giannozzi P, Cavazzoni C, Ballabio G, Scandolo S, Chiarotti G, Focher P, Pasquarello A, Laasonen K, Trave A, Car R, Marzari N, Kokalj A, http://www.pwscf.org/
40. Topsakal M, Cahangirov S, Ciraci S (2010) The response of mechanical and electronic properties of graphane to the elastic strain. Appl Phys Lett 96:091912
41. Monkhorst HJ, Pack JD (1976) Special points for Brillouin-zone integrations. Phys Rev B 13:5188–5192